

Diffusion in concentrated lattice gases: Intermediate incoherent dynamical scattering function for tagged particles on a square lattice

Ryszard Kutner

*Institut für Festkörperforschung der Kernforschungsanlage Jülich, D-5170 Jülich, Federal Republic of Germany
and Institute of Experimental Physics, University of Warsaw, Hoza 69, PL-00-681 Warsaw, Poland**

Klaus W. Kehr

*Institut für Festkörperforschung der Kernforschungsanlage Jülich, D-5170 Jülich, Federal Republic of Germany
(Received 27 January 1989)*

The time-dependent position self-correlation function of the particles of two-dimensional lattice gases was estimated by Monte Carlo simulations at various concentrations c . Two exponential decay modes were identified for $c < 0.5$ and three modes for $c > 0.5$ in the resulting intermediate incoherent dynamical scattering function. Published microscopic theories for that quantity are found to be at variance with the numerical results at larger wave vectors. A phenomenological description of the results is achieved by two-state models for $c < 0.5$ and three-state models for $c > 0.5$. A detailed physical interpretation of the model parameters, however, is an open question.

I. INTRODUCTION

The diffusion of tagged particles in lattice gases is interesting because of their correlated motion in a dynamical background. The long-range diffusion of tagged particles is now well understood through a series of theoretical papers.¹⁻⁶ The theoretical work was paralleled by various numerical simulations.^{6,7} This paper is directed to the analysis of the intermediate incoherent dynamical scattering function (intermediate IDSF). It is defined as the spatial Fourier transform of the position self-correlation function of particles and, hence, contains information on the tagged-particle motion over different length and time scales. The incoherent dynamical scattering function (IDSF), which is the Fourier transform of the position self-correlation function with respect to space *and* time, is experimentally accessible by incoherent inelastic scattering of neutrons.⁸ The intermediate IDSF as well as the IDSF were studied in several papers.^{3,4,9,10} As detailed below, the comprehension of these quantities is much less satisfactory than that of the long-range diffusion. The emphasis of this paper is on the analysis of numerical simulation results by phenomenological models, but also comparisons with the existing theories are made.

The main incentives for analyzing the simulation results on the intermediate IDSF of particles in lattice gases by phenomenological models were, first, the desire to better understand the physical mechanisms entering it, and second, the aim to contribute to the analysis of, especially, quasielastic neutron scattering experiments on hydrogen in metals. These systems are realizations of lattice gases; yet often the systems studied by experiments are more complicated than those treated by the formal theories.¹¹ One wants to understand the basic features observed in such experiments; this may be achieved by appropriate modeling.

One basic mechanism for correlations in the motion of

tagged particles in lattice gases was identified by Bardeen and Herring.¹² Suppose a particle made a transition to an empty neighboring site of the lattice at $t = 0$. Immediately after the transition, a vacancy is present at the site where the particle came from, whereas at the other neighbor sites vacancies are present according to the probability of occurrence of vacant sites. The presence of this "special vacancy" behind the tagged particle induces a backward correlation in its random walk. Bardeen and Herring were concerned with self-diffusion in metals, which is characterized by a small concentration $c_v \ll 1$ of vacant sites. The subsequent elaboration of this mechanism gave a complete description of the long-range diffusion of tagged particles in the limit $c_v \ll 1$.¹³ The Bardeen-Herring mechanism was used by van Beijeren and co-workers^{6,13} to also describe tagged-particle diffusion at arbitrary vacancy concentrations c_v . They stressed the role of the special vacancy in determining the velocity autocorrelation function of the tagged particle for general c_v . The formal theory based on these ideas⁶ is in excellent agreement with the simulations of the mean-square displacement (the equivalent theory of Tahir-Kheli⁵ is based on a different approach). It appears that the diffusion coefficient is indeed determined by the generalization of the Bardeen-Herring mechanism to arbitrary vacancy concentrations.

As will be discussed in this paper, the simple modeling of the intermediate IDSF of particles based on the backward correlations induced by the vacancies is not satisfactory. Model and simulations disagree at finite wave vectors. In a phenomenological picture of tagged-particle diffusion at arbitrary vacancy concentrations, the Bardeen-Herring mechanism is probably better characterized as a type of "blocking-induced backward correlation." Namely, when a tagged particle attempts to make a transition to an already occupied site, it cannot perform this transition. It turns out that the random blocking events of the tagged particle are dominant in determining

the intermediate IDSF. Expressed differently, at larger vacancy concentrations this function exhibits the typical features of a trapping model, not those of a backward-correlated one.

The investigations are restricted to lattice gases of arbitrary concentrations on the two-dimensional square lattice. One reason for this restriction is the better statistics which can be achieved in the numerical results in two dimensions, another one is the low coordination number ($z=4$) of the square lattice, which enhances correlation effects. An undesirable feature of the two-dimensional lattice is the recurrent nature of the random walk of tagged particles, resulting in logarithmic corrections to the mean-square displacement. The particles are assumed to be noninteracting; however, double occupancy of lattice sites is forbidden.

Section II contains the numerical simulations of the intermediate IDSF and its analysis. In Sec. III analytical theories are compared with the numerical simulations. Section IV describes the phenomenological modeling of the simulation results and Sec. V contains the concluding remarks.

II. NUMERICAL PROCEDURE

A. Monte Carlo simulations on square lattice

The hopping process of the tagged particles was numerically simulated by a modified standard Monte Carlo procedure. Since the standard procedure was comprehensively described in Ref. 10 for the case of tracer diffusion in a three-dimensional fcc lattice, as well as in the series of subsequent papers (for a review see Ref. 7), we only mention some special features and characteristic modifications used in the present approach.

The position self-correlation function $G_s(\mathbf{r}, t)$ of particles is defined, e.g., in Ref. 8. To estimate $G_s(\mathbf{r}, t)$ by simulations, we collected for given \mathbf{r} and t the events defined by $\mathbf{r} = \Delta \mathbf{r}_j(t)$, where $\Delta \mathbf{r}_j(t)$ is the difference between the actual position $\mathbf{r}_j(t)$ of the j th particle ($j = 1, \dots, N_p$, where N_p is the total number of particles) at time t and its initial one, $\mathbf{r}_j(0)$. In our simulations it was sufficient to assume that the distance $|\mathbf{r}|$ varies between 0 and 64 (the lattice constant is taken as unity), and the time t between 0 and 200 Monte Carlo steps/particle (MCS/p) at most. We also utilized the symmetry of the square lattice. The intermediate IDSF $I(\mathbf{k}, t)$ was calculated by a standard numerical cosine-Fourier transformation of the function $G_s(\mathbf{r}, t)$.

In order to systematically investigate the intermediate IDSF we performed numerical simulations for seven fixed particle concentrations, i.e., $c = 0.0998, 0.3005, 0.5008, 0.7010, 0.90, 0.952, \text{ and } 0.9805$. We typically used lattices with $N = 600 \times 600$ sites and for the longer runs 500×500 sites, and imposed periodic-boundary conditions. The main modification was introduced for $c > 0.5$. Namely, to achieve good statistics we used the vacancies instead of the particles to implement the hopping process in the lattice gas. In each Monte Carlo step a vacancy is selected at random, instead of a particle, as was done in the standard version of the program. Then, one of four

possible nearest-neighbor sites is selected at random. If this site is occupied by a particle the vacancy exchanges its actual position with the neighboring particle position. Exchange of two vacancies is excluded because such a process does not influence the dynamics of the particles. Since the initial and actual positions of all the particles and vacancies are monitored one can readily obtain quantities such as the time-dependent position self-correlation function of particles, $G_s(\mathbf{r}, t)$. In this procedure the discrete time t is directly measured in units of Monte Carlo steps per vacancy (MCS/v). It is seen that the average number of jumps performed by the vacancies and hence by the particles during 1 MCS/v equals $N(1-c)c$, where N is the total number of lattice sites. On the other hand, this is exactly the average number of jumps performed by the particles during 1 MCS/p in the standard version of the Monte Carlo simulations. Hence, both time units are completely equivalent. It is clear that the efficiency ratio between both approaches (i.e., the ratio between the number of attempted vacancy jumps during 1 MCS/v and the number of attempted particle jumps during 1 MCS/p) equals $(1-c)/c$ so that for $c > 0.5$ the new method is preferable while for $c < 0.5$ it is the old one.

B. Results of the simulations

The general result of the simulations is that the intermediate IDSF $I(\mathbf{k}, t)$ consists of several exponentially decaying functions. Some typical results of the numerical simulations are shown in Fig. 1; a particle concentration of $c = 0.7010$ was chosen and three different k values in the (1,1) direction. The main feature of the results is the exponential decay of $I(\mathbf{k}, t)$ with time for longer times. As the fitted straight lines indicate we observe a well-defined asymptotic decay described by a simple exponential function of time, this feature was found for all particle concentrations and wave vectors. For small k (e.g., $k = 0.430$ in the figure) the decay law is $\sim \exp(-D_{\text{tr}} k^2 t)$

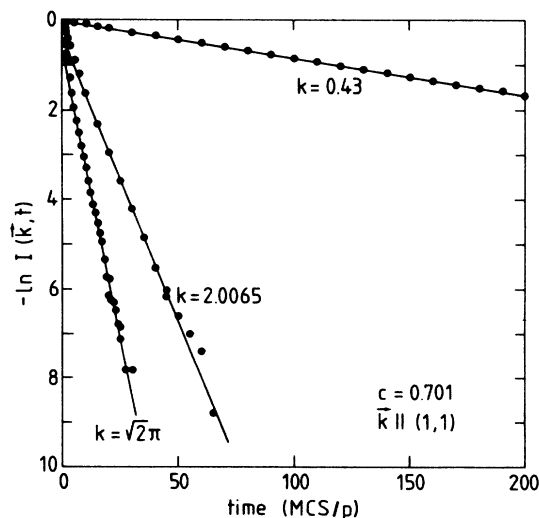


FIG. 1. Intermediate incoherent dynamical structure function as a function of time, for three values of the wave number. Double points at the same time are from different runs.

and D_{tr} agrees within the accuracy of the analysis with the tracer-diffusion coefficient at the corresponding concentration.

It is also seen from Fig. 1 that the intermediate IDSF cannot be described, for smaller times and larger k , by a single exponential function of time; there are deviations from the fit with a straight line. We analyzed these deviations systematically for all particle concentrations studied, as a function of the wave vector \mathbf{k} in the (1,1) direction. For $c=0.7010$, we investigated also \mathbf{k} in the (1,0) direction. The details of the analysis are shown in Figs. 2(a)–2(c) for $c=0.7010$, $k=2.0065$, and \mathbf{k} in the (1,1) direction. Figure 2(a) shows the complete time range covered for these parameters; not all data points are shown. A well-defined asymptotic behavior $I_1(\mathbf{k}, t) = W_1(\mathbf{k}) \exp[-R_1(\mathbf{k})t]$ can be extracted from the data, and is represented by the straight line. In Fig. 2(b)

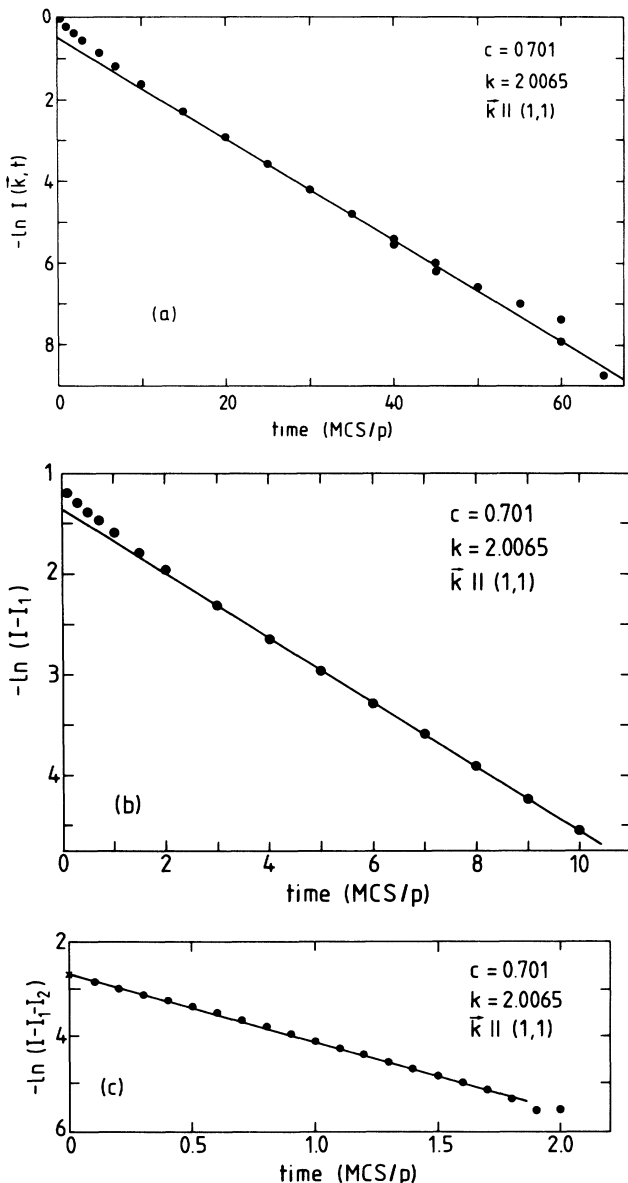


FIG. 2. Analysis of the intermediate incoherent dynamical structure function at $c=0.701$ as discussed in the main text.

we depict the logarithm of the difference $I(\mathbf{k}, t) - I_1(\mathbf{k}, t)$. We observe that there appears a time range, where this difference can again be represented by an exponential function, $I_2(\mathbf{k}, t) = W_2(\mathbf{k}) \exp[-R_2(\mathbf{k})t]$. The time range extends from relatively short times to the times where the difference $I - I_1$ is significantly above the statistical fluctuations of the data; it is an intermediate time in the scale of Fig. 2(a). The subtraction procedure is repeated once more in Fig. 2(c), where $\ln[I(\mathbf{k}, t) - I_1(\mathbf{k}, t) - I_2(\mathbf{k}, t)]$ is plotted. The difference $I - I_1 - I_2$ can be represented, over the whole remaining time range, by a single exponential, $I_3(\mathbf{k}, t) = W_3(\mathbf{k}) \exp[-R_3(\mathbf{k})t]$.

We thus observe that the intermediate IDSF can be decomposed, for this particular concentration and wave vector, into a sum of three simple exponential functions. The decomposition of the intermediate IDSF in three exponential functions was possible for all \mathbf{k} values at the concentrations of $c=0.5008$, 0.7010 , 0.90 , and 0.9502 . At the lower concentrations of $c=0.0998$ and 0.3005 only a decomposition into two exponential functions could be made, $I(\mathbf{k}, t) = W_1(\mathbf{k}) \exp[-R_1(\mathbf{k})t] + W_2(\mathbf{k}) \exp[-R_2(\mathbf{k})t]$. This is demonstrated in Figs. 3(a) and 3(b) for the case $c=0.3005$ and $k=2.0065$. The case $c=0.9805$ requires a separate discussion, since it is difficult for this case to decide between a decoupling into two or three components. The sum of the weights must

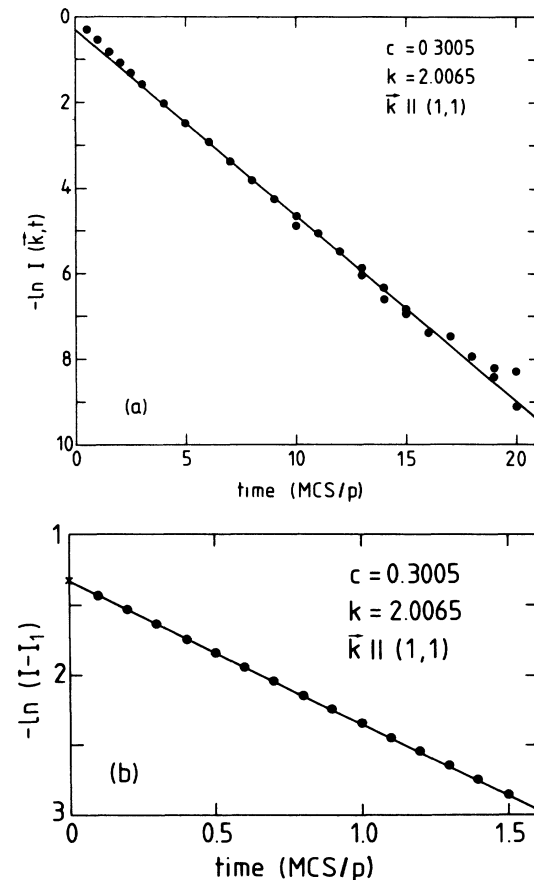


FIG. 3. Analysis of the intermediate incoherent dynamical structure function at $c=0.3005$ as discussed in the main text. Double points in (a) at the same time are from different runs.

be one at arbitrary \mathbf{k} . The crosses in Figs. 2(c) and 3(b) are determined by this condition. They agree well with the extrapolation of the fitted straight lines to $t=0$. We consider this agreement as an important self-consistency test.

The quantities $R_i(\mathbf{k})$ and $W_i(\mathbf{k})$ are plotted in Figs. 4(a) and 4(b), respectively, for $c=0.701$, \mathbf{k} in the (1,1) direction, and $i=1,2,3$. The Fourier transform of a sum of exponential functions in time consists of a sum of Lorentzians in the frequency domain whose widths are $R_i(\mathbf{k})$ and the corresponding weights $W_i(\mathbf{k})$, hence we will call the $R_i(\mathbf{k})$ widths and the $W_i(\mathbf{k})$ weights. A similar behavior as shown in Fig. 4 was found at the other concentrations above $c=0.5$. The dashed line in Fig. 4(a) represents the mean-field prediction for the width $R_2(\mathbf{k})$. Namely, the width function $R(\mathbf{k})$ of a particle performing uncorrelated random walk on a square lattice, in a background of other particles, is

$$R(\mathbf{k}) = (1-c)4\Gamma(1 - \frac{1}{2}\cos k_1 - \frac{1}{2}\cos k_2), \quad (1)$$

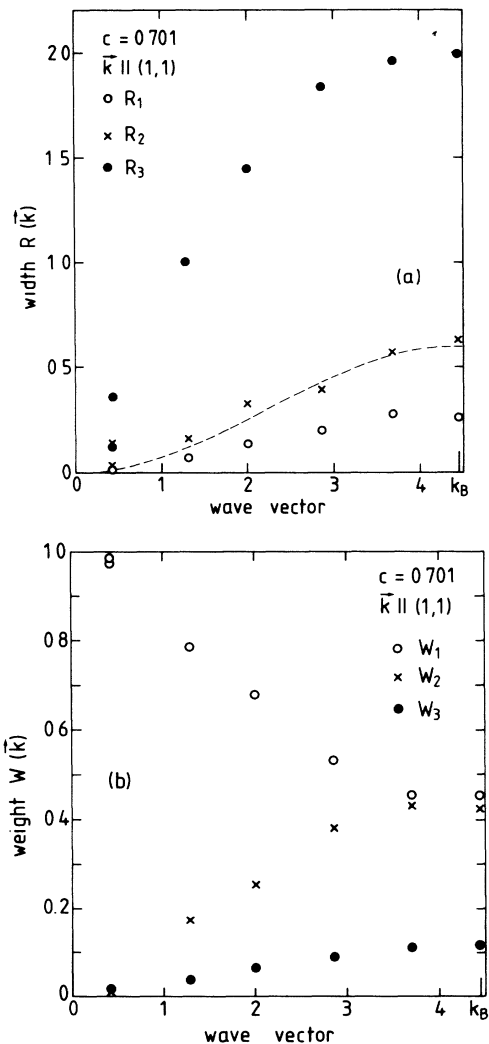


FIG. 4. Widths $R_i(\mathbf{k})$ and weights $W_i(\mathbf{k})$ deduced from the simulated intermediate IDSF at $c=0.701$, for different \mathbf{k} values. The dashed line in (a) represents mean-field behavior; cf. the main text.

where Γ is the transition rate between two sites and $(1-c)$ the average blocking factor. It is surprising that the intermediate width $R_2(\mathbf{k})$ is so well described by the mean-field expression (1). We made the same observation for all other particle concentrations above $c=0.5$. Figures 5(a) and 5(b) show $R_i(\mathbf{k})$ and $W_i(\mathbf{k})$ for $c=0.3005$, \mathbf{k} in (1,1) direction, where only two modes were identified. Generally, the mode with the lowest width $R_1(\mathbf{k})$ is the "diffusive mode," it behaves as $D_{tr}k^2$ for small k as already noted above. Also its weight approaches one for small k , as it should be.

A general relation for the widths and weights is obtained in the following way. The expansion of the intermediate IDSF for small time reads

$$I(\mathbf{k}, t) = 1 - \sum_i W_i(\mathbf{k}) R_i(\mathbf{k}) t + \dots \quad (2)$$

For short times, the behavior of a tagged particle should exhibit uncorrelated hopping in an average background, i.e., meanfield behavior. Hence, the coefficient of the

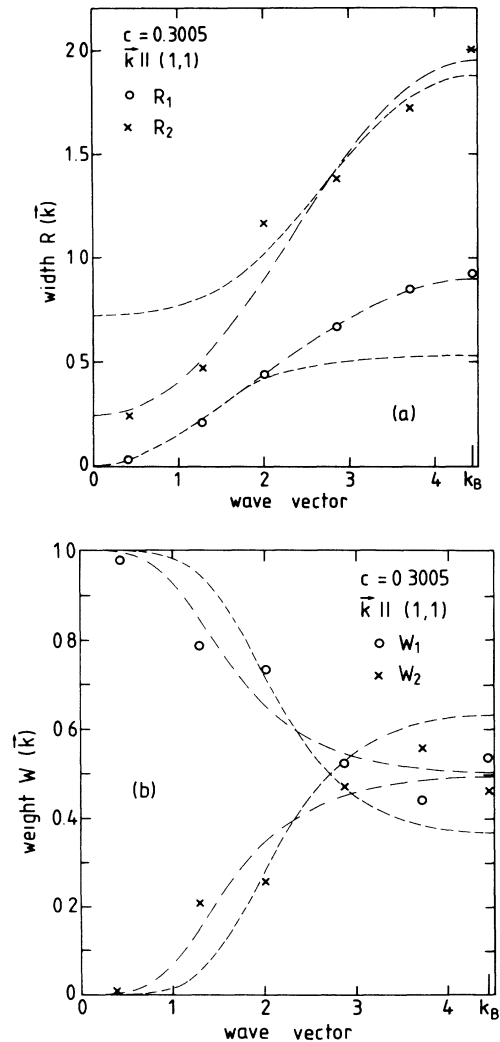


FIG. 5. Widths $R_i(\mathbf{k})$ and weights $W_i(\mathbf{k})$ deduced from the simulated intermediate IDSF at $c=0.3005$, for different \mathbf{k} values. The dashed and dashed-dotted lines are explained in Sec. IV.

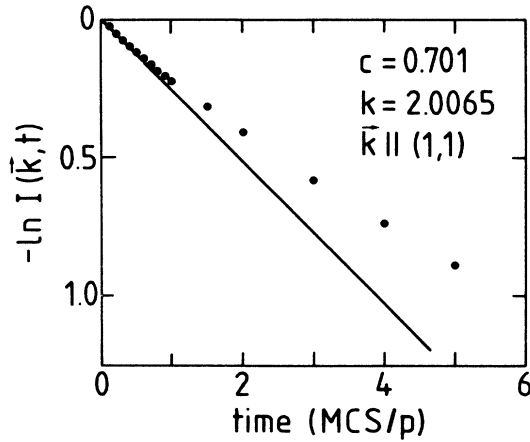


FIG. 6. Behavior of the intermediate IDSF as a function of time, for short times. The points represent simulation results and the line corresponds to the mean-field expression.

first-order term must be equal to the mean-field width $R(\mathbf{k})$ of the tracer particle in the lattice gas,

$$\sum_i W_i(\mathbf{k})R_i(\mathbf{k}) = R(\mathbf{k}). \quad (3)$$

This "sum rule" was well obeyed by the quantities $R_i(\mathbf{k})$ and $W_i(\mathbf{k})$ obtained at all concentrations. Further analysis of the behavior of $R_i(\mathbf{k})$ and $W_i(\mathbf{k})$ is made in the following sections.

Also, a numerical test on the initial-time behavior of the intermediate IDSF was made in the following way. According to (3), the intermediate IDSF is then given by $I_{MF}(\mathbf{k}, t) = \exp[-R(\mathbf{k})t]$ and the width $R(\mathbf{k})$ is given by (1). This expression has been plotted in Fig. 6 for $c = 0.701$ and $k_1 = k_2 = 2.0065/\sqrt{2}$, together with data points from the simulations. One recognizes very good agreement for short times; discrepancies appear for larger times. The same behavior was found at all other wave vectors and concentrations.

III. COMPARISON WITH ANALYTICAL THEORIES

Three groups developed analytical theories of tagged-particle diffusion in lattice gases in higher dimensions in the past. These theories had all the same starting point, namely, the master equation for the hopping diffusion of one tagged particle in a lattice gas, where the background particles also diffuse, and double occupancy of sites was excluded. The formal procedures used in these theories were very different. However, the physical approximations which were made appear to be identical; hence the results should be equivalent.

Fedders and Sankey¹ formulated a multiple-scattering approach by using diagrammatic methods. They included the repeated scattering of a tagged particle with one vacancy; the other background particles are treated in mean-field approximation. The results for the static correlation factor are not completely satisfactory. A correct form was given for simple-cubic lattices^{1,14} but

one parameter appearing in the theory was not properly identified. The result for the Laplace transform of the intermediate IDSF can be given in the form

$$I(\mathbf{k}, s) = [s + \Sigma(\mathbf{k}, s)]^{-1}, \quad (4)$$

where $\Sigma(\mathbf{k}, s)$ is called a self-energy or memory function. Fedders and Sankey give $D_i(\mathbf{q}, \omega)$; this quantity is obtained from $I(\mathbf{k}, s)$ by substituting $s = -i\omega$ and $\mathbf{k} = \mathbf{q}$. Their self-energy is designated by $K(\mathbf{q}, \omega)$ and it is expressed in terms of two auxiliary quantities, which are finally related to lattice Green functions. The relations involve only algebraic equations which are readily solved. We calculated the lattice Green functions numerically and solved the relations for the self-energy, keeping the Laplace variable s . Finally, the form (4) was transformed back into the time domain by numerically inverting the Laplace transform.¹⁵ The result is given in Fig. 7 for the typical concentration $c = 0.701$, together with the simulation data. One observes good agreement between simulations and theory at smaller k , but appreciable deviations at larger k .

Fedders and Sankey¹⁴ also provided an approximate form for the self-energy which we examined also. The form is, in our terminology,

$$\Sigma(\mathbf{k}, s) = R(\mathbf{k}) \left[1 - \frac{p_1}{p_2(\mathbf{k}) + s} \right], \quad (5)$$

where $R(\mathbf{k})$ is the width function of the intermediate IDSF of a tracer particle that performs an uncorrelated

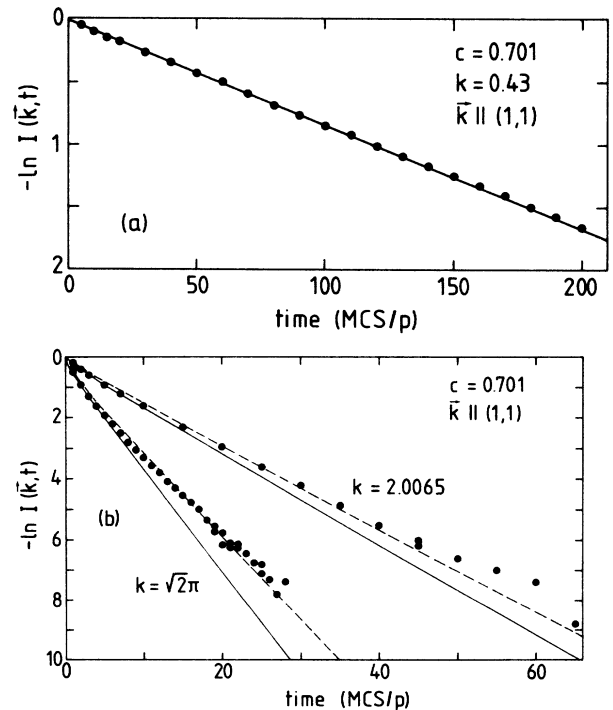


FIG. 7. Comparison between the simulation results for the intermediate IDSF and theory. Points, simulation results; dashed lines, simplified theory of Fedders and Sankey; solid lines, theories of Sankey and Fedders and of Tahir-Kheli (indistinguishable).

walk in the lattice gas. For the square lattice it was given by (1). It is required that the correct tracer-diffusion coefficient results for small k , $K(\mathbf{k}, 0) = f(c)R(\mathbf{k})$ for $k \rightarrow 0$, where $f(c)$ is the correlation factor. The empirical approximation $p_1 = 2c\Gamma$ does then determine $p_2(\mathbf{k})$, namely,

$$p_2(\mathbf{k}) = 2c[1 - f(c)]^{-1}. \quad (6)$$

As is obvious from (4) and (5) the approximate IDSF has two poles in the Laplace domain, or consists of a sum of two exponentials in the time domain. For small k there is only one diffusive pole with weight ≈ 1 . The comparison with the simulation data is included in Fig. 7, in form of the dashed lines. There is reasonable agreement for small k , at larger k this approximate form also does not give a correct description of the simulation results. The same holds for other concentrations and wave vectors. It is interesting to note that this approximate form of the IDSF yields better agreement with the numerical data than the original theory (solid line). Since the approximation was constructed in an *ad hoc* manner, one must consider this improvement as fortuitous.

A completely different approach was taken by Nakazato and Kitahara.² They studied the evolution of the system under the influence of a Liouville operator in a suitable occupation-number space and took $c(1-c)$ as their expansion parameter. They could obtain a frequency-dependent diffusion coefficient at arbitrary concentrations. From the static diffusion coefficient the following correlation factor is obtained:

$$f(c) = \frac{1 + \langle \cos\theta \rangle}{1 + [(2-3c)/(2-c)]\langle \cos\theta \rangle}, \quad (7)$$

where $\langle \cos\theta \rangle$ is the average angle between consecutive transitions of the tagged particle *in the limit* $c \rightarrow 1$. This quantity has been calculated exactly for various lattices, see, e.g., Ref. 16. The expression (7) agrees well with the simulation results, apart from small discrepancies, see below. Unfortunately, the complete IDSF was not derived by these authors.

Tahir-Kheli and Elliott³ approached the problem of tracer diffusion in lattice gases by studying the equation of motion for the position self-correlation function of (tagged) particles. There appears a hierarchy of coupled equations involving higher-order time-dependent occupancy correlation functions. These functions describe the occupancy of lattice sites by tagged particles, other particles, or vacancies. The hierarchy is decoupled by neglecting time-dependent occupancy correlation functions for one tagged particle and two vacancies, all being at different sites.³ The correlation factor obtained by Tahir-Kheli and Elliott is identical to the one given above (7); this implies that the approximations are equivalent to those made by Nakazato and Kitahara. They also identify a self-energy by writing the IDSF in the form (4), and they use $-i\omega$ instead of s . A more suitable form for an explicit calculation of the self-energy appears in a subsequent paper.⁴ Here $\Sigma(\mathbf{k}, s)$ is expressed in terms of an auxiliary quantity which is related to lattice Green functions by algebraic equations. We solved these equations, where we used numerically integrated lattice Green func-

tions and determined the intermediate IDSF $I(\mathbf{k}, t)$ in the time domain by numerical Laplace inversion. The result of this procedure turns out to be identical to the theory of Sankey-Fedders. The same remarks as made above also apply to this theory: good agreement for small k , appreciable discrepancies at finite wave vectors; cf. also Fig. 7. The general conclusion is that this class of theories does not yet give a satisfactory description of the intermediate IDSF at general wave vectors.

Recent improvements of the theory of tagged-particle diffusion in lattice gases were made by Tahir-Kheli⁵ and van Beijeren and Kutner.⁶ Tahir-Kheli treated the correlated vacancy-tracer diffusion in the frame of his theory in a self-consistent fashion. This is especially important when the background particles have a different (smaller) transition rate. van Beijeren and Kutner provide a fourth variant of the theory of tagged-particle diffusion by investigating the stochastic process of return of the special vacancy to the tracer. This is the vacancy which has made the original exchange with the tagged particle. As pointed out by them, only the subsequent exchanges of the tracer with this vacancy can lead to correlation effects in the diffusion. Hence their theory can be considered as a generalization of the original theory of Bardeen and Herring¹² to lattice gases of arbitrary concentrations. Also in their theory the correlated vacancy-tracer motion is determined self-consistently, and the results are identical with those of Ref. 5. The results give an improved and excellent agreement with the data on the asymptotic mean-square displacement and its correction in $d=2$.⁶ The improved theories of Tahir-Kheli, van Beijeren, and Kutner have not yet been extended to the self-correlation function of particles for arbitrary times. It is an open question whether such an extension will result in an improved theoretical description of this quantity.

IV. PHENOMENOLOGICAL MODELS

In Sec. III we arrived at the conclusion that the theoretical understanding of the intermediate IDSF for lattice gases at arbitrary concentrations is still rather unsatisfactory, despite the various theoretical efforts. In this section we wish to interpret the behavior of the intermediate IDSF as revealed by the simulations in terms of phenomenological models. We shall first describe some simplified models, and comment on other, partially phenomenological approaches.

One simple model for tagged-particle diffusion in the limit of small vacancy concentration is the *encounter model*, which was originally developed in the NMR context.¹⁷ It is based on the fact that a vacancy makes, on the average, only a few exchanges with the tagged particle and disappears afterwards.¹⁸ Wolf¹⁹ applied this model to the derivation of the IDSF. The resulting intermediate IDSF consists of a single exponential; only the width is more complicated as a function of \mathbf{k} than in mean-field theory. While the long-time behavior of the simulated intermediate IDSF can be described correctly by this model, the short-time behavior is not correct. Also the extension to larger vacancy concentrations is not obvious.

Ross and Wilson⁹ determined the IDSF by calculating

$G_s(\mathbf{r}, t)$ as a sum of the contributions with a given number n of attempted transitions. The temporal probability for n attempted transitions follows from the assumption of a Poisson process; the probabilities for the spatial distribution of the tagged particle after n steps are determined by the simulations. It is clear that a phenomenological representation of the IDSF is achieved by this method; however, the physical meaning of the spatial probabilities after n steps remains unclear.

A candidate for the phenomenological description of the intermediate IDSF of lattice gases seems to be the simple *backward jump model*, where the tagged particle has a larger than average rate for jumps in the backward direction and smaller rates for jumps in forward or sideward directions. For a general description of correlated jump models see Ref. 20. The backward jump model would incorporate in a natural manner the existence of the backward correlations that are expressed by the correlation factor $f(c)$. However, the width and weight structure that we observed in the simulations at finite concentrations c are not in agreement with the predictions of the backward jump model. First, the backward jump model yields only two decay modes while we found three decay modes at concentrations $c > 0.5$. Second, the behavior of the widths and weights as a function of \mathbf{k} , as deduced from the simulations, is more similar to the behavior of a *trapping model* than to the backward jump model. This becomes evident by a comparison of Figs. 4 and 5 with the Figs. 5.2(a) and 5.2(b) of Ref. 20. We also tried to fit the backward jump model to the intermediate IDSF in the time domain but we found severe discrepancies.

An extension of the simple backward jump model is a model where general, distinct, waiting-time distributions are used for the individual steps. This extension was developed by Kehr, Kutner, and Binder.¹⁰ They determined the waiting-time distributions by numerical simulations and analyzed them in terms of the stochastic processes that occur in tagged-particle diffusion. The authors then derived the IDSF in the frame of the general backward jump model, and gave explicit results for it where the previously determined waiting-time distributions were used. This approach seems to give a correct description of the IDSF in the frequency domain for fcc lattices. However, the backward jump model with general waiting-time distributions is rather complicated, as well as the structure of the waiting-time distributions themselves. Thus no practical description of the IDSF is obtained by this procedure. An open question is whether

the model assumption of a memory between two successive steps of the tracer atom only, does also hold for lattices with lower coordination numbers. Deviations from this assumption were observed in the honeycomb lattice.²¹

We now describe the simulation results at smaller concentrations in terms of two-state models. As noted above the behavior of the widths $R_i(\mathbf{k})$ and weights $W_i(\mathbf{k})$ as shown in Fig. 5 is similar to those models. In the two-state model, the particle is alternatively in state (1) where it performs an uncorrelated random walk with rate γ_1 , or in state (2) where it may perform a random walk with rate γ_2 . If $\gamma_2=0$, then we have the trapping model. The transitions between the states are characterized by the rates γ_t for transitions to state (2) and γ_r for release from that state. Explicit expressions are given in Ref. 20.

When simulation data are compared with a model the question arises whether a fit should be made in the time or frequency domain. A fit of the simulation results for the intermediate IDSF in the time domain would be more direct, and it would give stronger weight to the long-time or low-frequency behavior. We decided to use the widths $R_i(\mathbf{k})$ and weights $W_i(\mathbf{k})$ that were extracted from the simulation data, for the fit to the models. In this way we gave stronger emphasis to the high-frequency behavior. Here we had in mind the possible comparison with incoherent neutron scattering results. The actual fits were made simultaneously for the widths and weights at the \mathbf{k} values as shown in Fig. 5 for $c=0.3005$; analogous fits were made for $c=0.0998$. The results of the fits for $c=0.3005$ are indicated in Fig. 5 for the trapping model ($\gamma_2=0$) with dashed lines, and for the two-state model ($\gamma_2 \neq 0$) with dashed-dotted lines. One recognizes fair agreement between the simulation results and the trapping model, and very good agreement with the general two-state model.

The following physical picture emerges from the analysis. A tagged particle in a lattice gas at low concentrations performs an uncorrelated random walk until it hits another particle. It is then immobilized when it attempts to move in the direction of that particle. This "trapping event" is rather transient; already in the next step the particle may be free, or it may escape. In contrast, in a backward jump model the particle has always a tendency for backward jumps. The results of the fit for both models are given in Table I, at two concentrations. The parameters of the trapping model appear to be reasonable, especially at the lower concentration. The

TABLE I. Fit parameters of the trapping and two-state models at two different concentrations. The quantities γ_{eff} are derived from the other parameters.

	Trapping $c=0.0998$	Two-state $c=0.0998$	Trapping $c=0.3005$	Two-state $c=0.3005$
γ_1	1.0177	1.1019	0.8419	0.9175
γ_2	0	0.6140	0	0.3813
γ_t	0.1439	0.1825	0.1301	0.0949
γ_r	1.0804	0.2940	0.5923	0.1480
γ_{eff}	0.8981	0.9151	0.6903	0.7080

transition rate in the free state is near unity, and the trapping rate is much smaller than the release rate from the immobile state. However, we would have expected an increase of the trapping rate with concentration and an approximately constant release rate. An effective transition rate can be defined by

$$\gamma_{\text{eff}} = \gamma_1 \frac{\gamma_r}{\gamma_r + \gamma_t} + \gamma_2 \frac{\gamma_t}{\gamma_r + \gamma_t}. \quad (8)$$

It corresponds to the effective number of transitions to different sites per unit time. We observe that γ_{eff} is approximately $1 - c$; this is a plausible result. In the trapping and the two-state model the diffusion coefficient is also given by γ_{eff} since the random walk is uncorrelated. As a consequence, the diffusion coefficient deduced from the parameters will be too large (the correlation factor is missing) and the model prediction of the intermediate IDSF at small k will deviate from the simulation results. This is a consequence of the fact that we fitted the widths $R_i(k)$ and weights $W_i(k)$, which gives preference to the high-frequency behavior. The physical interpretation of the fit parameters of the two-state model is not obvious. In particular, we cannot associate the rate of transitions γ_2 in state (2) with a clear physical picture. It is satisfying that the effective transition rate is again $1 - c$, within the scatter of the data.

The results of the trapping and the two-state models for the intermediate IDSF $I(\mathbf{k}, t)$ are shown in Fig. 8 for $c = 0.3005$ at two \mathbf{k} values where the parameters of Table I were used. At the intermediate k value the predictions of both models are almost identical and agree well with the numerical data. For k at the Brillouin-zone boundary k_B , the prediction of the trapping model deviates from the simulation data at larger times, whereas the two-state model yields a satisfactory description. The deviation for $k = k_B$ is a consequence of the strong discrepancy between the fitted and the simulated values of the widths $R_i(k)$ at this k value. Of course we could also perform a fit in the time domain. This would then lead to better agreement at larger times but to larger discrepancies at shorter times. In summary, the two-state model yields a

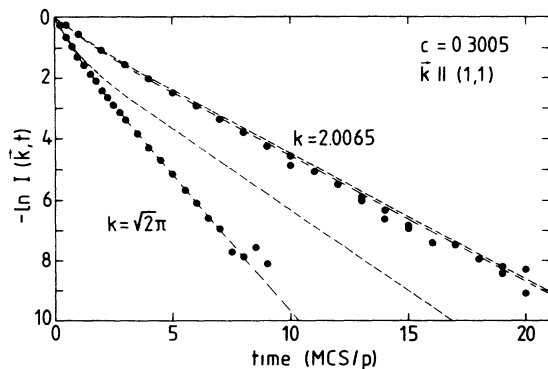


FIG. 8. Comparison between the simulation results for the intermediate IDSF and model predictions. Points, simulation results; dashed lines, trapping model; dashed-dotted lines, two-state model.

good description of the observed behavior of the incoherent intermediate IDSF at smaller concentrations.

We now turn to the interpretation of the simulation results at $c = 0.7010$ by phenomenological models. As discussed in Sec. II and shown in Figs. 2(a)–2(c) the intermediate IDSF exhibits three decay modes with three associated weights. Comparison of Figs. 4(a) and 4(b) with Figs. 5(a) and 5(b) of the review²⁰ shows that even at the higher concentration the general behavior of the widths and weights as functions of k is analogous to that of a trapping model and not to the backward-correlated jump model.

We analyzed the simulation data essentially by two different models.

(i) In a so called “combined model” the tagged particle is alternatively in one of the following states: In the first state, the particle performs a correlated random walk with Γ_f the rate for jumps in forward or sideward directions, and with Γ_b the rate for backward jumps. The backward correlations dominate, thus $\Gamma_b > \Gamma_f$. Instead of the rates Γ_b, Γ_f we use as parameters the summary transition rate $\gamma_1 = 3\Gamma_f + \Gamma_b$ and the parameter $\epsilon = (\Gamma_b - \Gamma_f)/\gamma_1$. In the second state, the particle performs uncorrelated motion with a summary jump rate γ_2 to neighbor sites. This jump rate may also be zero, then the particle is immobile in the second state. The transition rate from the backward correlated state (1) to the uncorrelated state (2) shall be η and the rate from state (2) to state (1) shall be α , both rates are parameters of the model.

This model was motivated by the following considerations. First, the model yields three decay modes, thus it is a candidate for the description of the simulation results at higher concentrations. Second, the general picture of the encounter model seems to be plausible at large concentrations, namely, that the tagged particle stays virtually immobile for random periods, interrupted by strongly correlated exchanges with vacancies.

(ii) The second model that we employed is a three-state model where the particle performs a random walk on the lattice with different transition rates in each of the states. In principle, transitions between each of the states are admitted. For practical reasons two transition rates between states were set equal to zero, see below. It is easy to set up and solve the master equations of these models, see, e.g., the review.²⁰

TABLE II. Fit parameters of the combined model and the three-state model for $c = 0.7010$. The parameters γ_{31} and γ_{23} were set equal to zero, and γ_{eff} are derived quantities.

Combined model	Three-state model
$\gamma_1 = 0.8935$	$\gamma_1 = 0.2005$
$\gamma_2 = 0.1247$	$\gamma_2 = 0.0630$
$\epsilon = 0.2319$	$\gamma_3 = 0.0244$
$\eta = 0.0198$	$\gamma_{12} = 0.2588$
$\alpha = 0.0107$	$\gamma_{13} = 0.2521$
	$\gamma_{21} = 0.1381$
	$\gamma_{32} = 0.0618$
$\gamma_{\text{eff}} = 0.3944$	$\gamma_{\text{eff}} = 0.2996$

Both models were fitted to the numerical results on the widths $R_i(\mathbf{k})$ and the weights $W_i(\mathbf{k})$; a simultaneous fit of all quantities at the different k values was made. The resulting parameters of the fit are given in Table II. As Figs. 9(a) and 9(b) demonstrate, the combined model cannot well describe the simulation results on $R_i(\mathbf{k})$ and $W_i(\mathbf{k})$. Also the average transition rate, defined by a generalization of (8), does not agree with the expected value $1 - c$. The typical features of a backward-correlated model, namely, a mode with large width at all k values, and the vanishing of a weight at the Brillouin-zone boundary k_B , are not present in the simulation data. By contrast the three-state model does provide a good fit of the numerical data on $R_i(\mathbf{k})$ and $W_i(\mathbf{k})$. Two parameters of this model were set equal to zero, after a provisional fit with nine parameters showed them to be small and rather uncertain. Since in the three-state model two more parameters were used than in the combined model, a better agreement with the data could be expected. In any case, the model does describe the essential features of the nu-

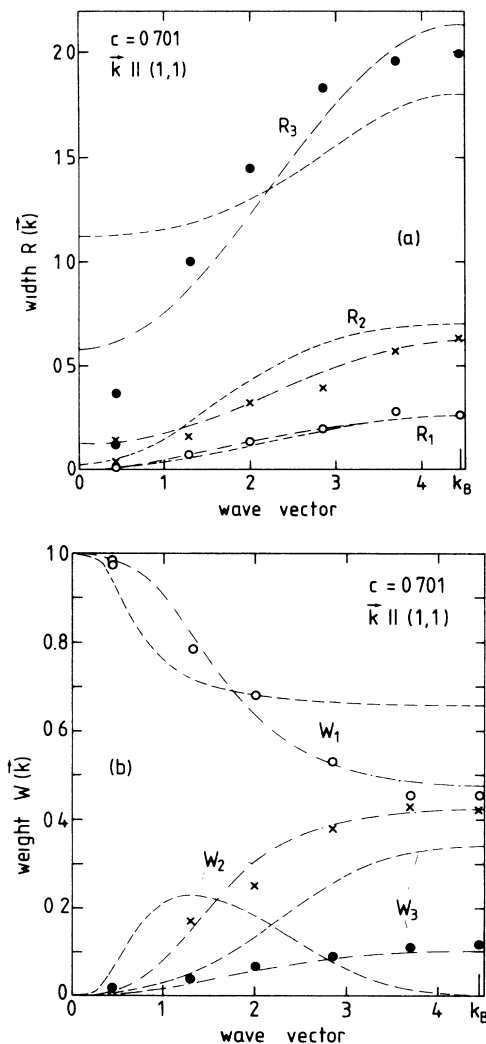


FIG. 9. Fit of the widths $R_i(\mathbf{k})$ and weights $W_i(\mathbf{k})$ by phenomenological models. Symbols, results extracted from the simulations; dashed lines, the combined model; dashed-dotted lines, three-state model.

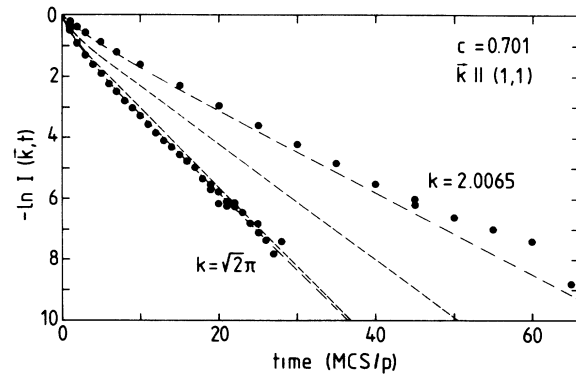


FIG. 10. Comparison between the simulation results for the intermediate IDSF and model predictions. Points, simulation results; dashed lines, the combined model; dashed-dotted lines, three-state model.

merical data. The point is that we cannot associate an obvious physical interpretation with the three different states and the transition rates between them. One satisfactory feature of the fit is that the average transition rate is again $1 - c$ within the numerical accuracy.

Finally, Fig. 10 shows the prediction of both models for the intermediate IDSF in the time domain, when the parameters of Table II are used. We observe that the combined model does not provide a good fit of the data, in particular at the intermediate k value. In contrast, the three-state model gives a very satisfactory description of the data in the time domain.

We also made a fit of the simulation data to the combined model *in the time domain*. This fit was satisfactory (remember that this procedure gives stronger weight to the long-time behavior), but the resulting widths and weights were then very different from the ones that were deduced from the numerical data.

In summary, we can fit the behavior of the widths and weights of the intermediate IDSF at the higher concentration $c = 0.7010$ quite well by a three-state model, similar to the lower concentrations, where a satisfactory fit was achieved with a two-state model. The physical meaning of the model and its parameters is unknown at present.

V. CONCLUSION

In this study we have estimated the space- and time-dependent position self-correlation function of the particles in two-dimensional lattice gases by numerical simulations. The intermediate IDSF was then obtained by a spatial Fourier transform. The analysis of this quantity showed the existence of two decay modes at concentrations $c < 0.5$ and of three decay modes at concentrations $c > 0.5$. The decay parameters (or widths of the corresponding Lorentzians in the frequency domain) and the associated weights were determined for several wave numbers.

The numerical results for the intermediate IDSF were compared with formal theories of that quantity. There are discrepancies between the simulation results and the predictions of those theories. Evidently there is a need

for more refined microscopic theories of the position self-correlation function in lattice gases.

One major aim of this study was the interpretation of the simulation results by phenomenological models. In this respect we were only partially successful. We could well describe the numerical results by two-state models for $c < 0.5$ and by three-state models for $c > 0.5$. However, the parameters of these models lack a physical interpretation. In other words, no consistent physical picture could be found which would allow a direct interpretation of the data. The obvious models for the tagged-particle motion in lattice gases, namely, the model of backward correlated jumps, and its combination with temporary transitions to a less mobile state, do not lead to a consistent description of the numerical data. One point seems to emerge from the analysis. Namely, the time-dependent mechanism of backward-correlated motion of tagged particles is more similar to a transient trapping picture, at arbitrary concentrations of the lattice gas, than to the picture of backward correlation at each step of a tagged particle. One particular feature, which is not understood, is the mean-field-type behavior of one of the widths at $c > 0.5$. One may say that one portion of the particles performs an uncorrelated, mean-field-type motion. However, the weight of this mode is k depen-

dent; hence there is coupling to the other modes. This coupling should result in hybridization with the other modes.

We omitted concentrations very near to one from our study. This region deserves a detailed investigation. In the limit $c \rightarrow 1$, the waiting-time distributions for tagged-particle transitions can be calculated exactly, extending, for instance, the approach of Benoist, Bocquet, and LaFore.²² It is a question of interest whether a complete description of the intermediate IDSF can be achieved at least for this regime.

Note added in proof. The ISDF was studied by Monte Carlo simulations for lattice gases on the tetrahedral sites of a bcc lattice by Faux and Ross.²³ Their work included several blocking conditions, namely no double occupancy, as well as blocking to the first, second, and third neighbors, respectively.

ACKNOWLEDGMENTS

We benefitted from discussions with R. Hempelmann and K. W. Schroeder. One of us (R.K.) was supported in part by the facilities of the Polish Ministry of National Education, under Project No. CPBP-01-06 and No. RPBR-RRI-14.

*Permanent address.

¹P. A. Fedders and O. F. Sankey, *Phys. Rev. B* **15**, 3580 (1977);

O. F. Sankey and P. A. Fedders, *ibid.* **15**, 3586 (1977).

²K. Nakazato and K. Kitahara, *Prog. Theor. Phys.* **64**, 2261 (1980).

³R. A. Tahir-Kheli and R. J. Elliott, *Phys. Rev. B* **27**, 844 (1983).

⁴R. A. Tahir-Kheli, *Phys. Rev. B* **27**, 6072 (1983).

⁵R. A. Tahir-Kheli, *Phys. Rev. B* **28**, 3049 (1983).

⁶H. van Beijeren and R. Kutner, *Phys. Rev. Lett.* **55**, 238 (1985).

⁷For a review, see K. W. Kehr and K. Binder, in *Applications of the Monte Carlo Method in Statistical Physics*, Vol. 36 of *Topics in Current Physics*, edited by K. Binder (Springer, Berlin, 1984), pp. 181 ff.

⁸L. Van Hove, *Phys. Rev.* **95**, 249 (1954).

⁹D. K. Ross and D. T. L. Wilson, in *Neutron Inelastic Scattering, 1977, Proceedings of the International Atomic Energy Agency, Vienna, 1977* (IAEA, Vienna, 1978), Vol. II, p. 383.

¹⁰K. W. Kehr, R. Kutner, and K. Binder, *Phys. Rev. B* **23**, 4931 (1981).

¹¹For some examples see the review article by R. Hempelmann, *J. Less-Common Met.* **101**, 69 (1984).

¹²J. Bardeen and C. Herring, in *Imperfections in Nearly Perfect*

Crystals, edited by W. Shockley (Wiley, New York, 1952), p. 261.

¹³See H. van Beijeren and K. W. Kehr, *J. Phys. C* **19**, 1319 (1986), and the references contained therein.

¹⁴P. A. Fedders and O. F. Sankey, *Phys. Rev. B* **18**, 5938 (1978), see also O. F. Sankey and P. A. Fedders, *ibid.* **20**, 39 (1979); **22**, 5135 (1980).

¹⁵G. Honig and U. Hirdes, *J. Comput. Appl. Math.* **10**, 113 (1984).

¹⁶M. Koiwa and S. Ishioka; *J. Stat. Phys.* **30**, 477 (1983).

¹⁷D. Wolf, *Phys. Rev. B* **10**, 2710 (1974).

¹⁸There are subtleties associated with the return processes of the vacancies and its influence on tracer motion, depending on the dimensionality of the system. These points are discussed in detail in Ref. 13.

¹⁹D. Wolf, *Solid State Commun.* **23**, 853 (1977).

²⁰J. W. Haus and K. W. Kehr, *Phys. Rep.* **150**, 263 (1987).

²¹R. Kutner, *J. Phys. C* **18**, 6323 (1985).

²²P. Benoist, J. L. Bocquet, and P. LaFore, *Acta Metall.* **25**, 265 (1977).

²³D. A. Faux and D. K. Ross, *J. Less-Common Met.* **129**, 229 (1987).